Exploring Correlation-Based Brain Networks with Adaptive Signed Random Walks

Roberto C. Sotero[1], Jose M. Sanchez-Bornot[2]

[1] Department of Radiology, and Hotchkiss Brain Institute. University of Calgary, Calgary, AB, Canada.
[2] Intelligent Systems Research Centre, Ulster University, Derry Londonderry, United Kingdom

Corresponding Author:
Roberto C. Sotero[1]
HSC 2923 - 3330 Hospital Drive NW, Calgary, AB, T2N 4N1, Canada
Email address: roberto.soterodiaz@ucalgary.ca

Abstract

The human brain is a highly connected network with complex patterns of correlated and anticorrelated activity. Analyzing functional connectivity matrices derived from neuroimaging data can provide insights into the organization of brain networks and their association with cognitive processes or disorders. Common approaches, such as thresholding or binarization, often disregard negative connections, which may result in the loss of critical information. This study introduces an adaptive random walk model for analyzing correlation-based brain networks that incorporates both positive and negative connections. The model calculates transition probabilities between brain regions as a function of their activities and connection strengths, dynamically updating probabilities based on the differences in node activity and connection strengths at each time step. Results show that the classical random walk approach, which considers the absolute value of connections, overestimates network integration and segregation while underestimating the mean first passage time (MFPT) compared to the proposed adaptive random walk model. The adaptive model captures a wide range of interactions and dynamics within the network, providing a more comprehensive understanding of its structure and function. The study suggests that considering both positive and negative connections, has the potential to offer valuable insights into the interregional coordination underlying various cognitive processes and behaviors.

Introduction

The human brain is an intricate and highly connected network, with numerous regions displaying complex patterns of correlated and anticorrelated activity (Bressler and Menon 2010). Functional connectivity matrices (Friston 1994) represent the statistical relationships between these activity signals from different brain regions, often derived from neuroimaging data such as functional Magnetic Resonance Imaging (fMRI), Electroencephalography (EEG), or Magnetoencephalography (MEG). These matrices can be used to investigate the organization of brain networks and to identify patterns of connectivity associated with different cognitive processes or brain disorders by means of various analytical techniques, such as graph theory and complex network analysis (Bassett and Sporns 2017; Bullmore and Sporns 2009).

When performing complex network analysis on correlation-based functional connectivity matrices, one of the following approaches is typically used: 1) Thresholding: where we apply a threshold to the functional connectivity matrix, preserving only the connections with correlations above a certain value (often positive correlations) (van den Heuvel and Hulshoff Pol 2010; Kazeminejad and Sotero 2019). This way, we create a binary or weighted network, discarding the negative correlations. This approach can lead to a loss of information about the negative interactions between brain regions (Rubinov and Sporns 2011). 2. Binarization: this involves binarizing the functional connectivity matrix by assigning "1" to connections with correlations above a specified threshold and "0" to connections below the threshold (Bassett and Sporns 2017; Kazeminejad and Sotero 2019). This approach also discards the negative correlations and can be used for further network analysis on a binary network. 3. Separate analysis of positive and negative connections. Two networks are created – one for positive correlations and another for negative correlations – and then perform network analysis on each network independently. This approach preserves the information about negative interactions between brain regions but treats them as separate entities (Sotero et al. 2020). 4. Disregard information about the connection sign by taking the absolute value of the connections (Meszlényi et al. 2017; Mahadevan et al. 2021). By disregarding the sign of the connections, we may inadvertently overlook critical aspects of the brain's organization, such as the balance between correlated and anticorrelated activity, which can provide insight into the interregional coordination underlying various cognitive processes and behaviors.

One approach that has shown promise in exploring the structure of complex networks, is the use of random walks (Noh and Rieger 2004). Random walks represent a type of stochastic process that characterizes the random motion of an object or particle in either discrete or continuous spaces (Pearson 1905). Within graph theory and network analysis, random walks are frequently employed to model the movement of a "walker" on a graph, with the walker traversing from one node to another along the edges of the graph (Riascos and Mateos 2021). Random walks have been adapted for use with signed social networks by adjusting the transition probabilities to preferentially favor positive edges over negative edges, or vice versa (Wan et al. 2019; Zhou et al. 2018; Yang, Cheung, and Liu 2007). However, the interpretation of signed connections in social networks, in terms of "trust" and "distrust", as well as the associated

transition probability models, are not directly transferable to correlation-based brain networks. As such, a signed random walk model that aligns with the physiological interpretation of correlated and anticorrelated activity in the brain is necessary.

In this study, we introduce a novel adaptive random walk approach to analyze correlation-based brain networks, investigating the transition probabilities between nodes (brain regions) as a function of their activities and connection strengths. The distinguishing feature of this model is the inclusion of both positive and negative connections when calculating transition probabilities. Positive connections signify an increased probability of transition between nodes exhibiting similar activities, while negative connections denote a higher likelihood of transition between nodes with dissimilar activities. By dynamically updating the transition probabilities in response to node activity differences at each time step and considering connection strengths, the adaptive random walk model offers a more comprehensive insight into the network's efficiency.

Our findings indicate that the classical random walk approach, which considers the absolute value of connections, overestimates network integration (measured by global efficiency) and segregation (measured by the average of local efficiencies) while underestimating the mean first passage time (MFPT) compared to our adaptive random walk, which considers both positive and negative connections. This proposed method captures a wide range of interactions and dynamics within the network, providing a more comprehensive understanding of its structure and function.

Materials & Methods

Computing the functional connectivity matrices

In this study, resting-state (rs)-fMRI data from 491 neurotypical subjects were obtained from the ABIDE Preprocessed Initiative (Cameron, Yassine, et al. 2013). To ensure that our results were not influenced by any custom preprocessing pipeline, we utilized the preprocessed data provided by ABIDE in the C-PAC pipeline (Cameron, Sharad, et al. 2013). The preprocessing involved several steps. First, the skull was removed from images using the Analysis of Functional Neuro Images (AFNI) software (Cox 1996). The brain was then segmented into three tissues using FMRIB Software Library (FSL) (Smith et al. 2004) and the images were normalized to the MNI 152 stereotactic space (Grabner et al. 2006; Mazziotta et al. 2001) using Advanced Normalization Tools (ANTs) (Avants et al. 2011). Functional preprocessing included motion and slice-timing correction, as well as voxel intensity normalization. Nuisance signal regression was also performed, which encompassed 24 parameters for head motion, CompCor (Behzadi et al. 2007) with five principal components for tissue signal in cerebrospinal fluid and white matter, and linear and quadratic trends for low-frequency drifts. Global signal regression (GSR) was applied to remove the global mean from signals, and images were co-registered with their anatomical counterparts using FSL. Subsequently, the images were normalized to the MNI 152 space using ANTs.

The average voxel activity in each Region of Interest (ROI) of the anatomical automatic labelling (AAL) atlas (Tzourio-Mazoyer et al. 2002) was extracted as the time series for that region. As rs-fMRI primarily focuses on low-frequency fluctuations (< 0.1 Hz), a bandpass filter

was applied to frequencies between 0.01 Hz and 0.1 Hz. To construct the brain network, the time series for each atlas ROI were correlated with the other regions using Pearson correlation. The strengths of these correlations were used as the connection strengths between different ROIs. In graph terms, this represents a graph where each node is at the center of the corresponding ROI, and each edge weight corresponds to the correlation between the two nodes at opposite ends of the edge.

Walk rule on the correlation network

First, let us consider an unweighted network consisting of N nodes. We place a large number (K) of random walkers onto this network, where K is significantly larger than N. At each time step, the walkers move randomly between the nodes that are directly linked to each other, with equal probability. We allow the walkers to perform T time steps, and as a walker visits a node, we record the number of walkers in the node. After T time steps, we expect that nodes with high degree (hubs) will have a higher number of walkers than nodes with low degree.

For weighted networks, such as the functional connectivity matrix representing the brain network, we propose a routing strategy that takes into account the sign of the connection. In the proposed random walk model for correlation networks, the transition probabilities are computed based on the weights in the functional connectivity matrix (C) and a similarity measure between the activities of the source and destination nodes. The main idea is to favor transitions between nodes with similar activities while also considering the positive or negative weights in the network. Specifically, the transition probabilities are computed as follows:

1. At each time step t, we compute the activity $A(i,t)$ (number of walkers) at each node i.
2. For each node i, we calculate the adjusted weights for all its neighboring nodes j as follows:
   a. We introduce the similarity measure $S_{ij}(t)$ between the activity of node i and node j at time t using the formula:

$$S_{ij}(t) = 1 - \left|\frac{A_i(t) - A_j(t)}{\max\,(A_i(t), A_j(t))}\right| \tag{1}$$

To normalize the difference between the activities of the nodes, we divide by the maximum of the activities $\max\,(A_i(t), A_j(t))$. The similarity $S_{ij}(t)$ ranges between 0 and 1. A value closer to 1 indicates that the activities of nodes i and node j more similar, while a value closer to 0 indicates that the activities are more dissimilar.

   b. If the weight C_{ij} is positive, the adjusted weight is:

$$\tilde{C}_{ij}(t) = C_{ij} S_{ij}(t) \tag{2}$$

If the weight C_{ij} is negative, the adjusted weight is:

$$\tilde{C}_{ij}(t) = |C_{ij}|\left(1 - S_{ij}(t)\right) \tag{3}$$

3. We then calculate the sum of the adjusted weights for all neighbors of node i. The transition probability $P_{ij}(t)$ from node i to each neighboring node j is computed as:

$$P_{ij}(t) = \tilde{C}_{ij}(t) / \sum_{j=1}^{N} \tilde{C}_{ij}(t) \tag{4}$$

Thus, a walker is more likely to travel through a positive connection C_{ij} if the activities in nodes i and j are similar, while it is more likely to take a negative connection if the activities are dissimilar.

Topological measures for correlation-based brain networks based on random walks

Efficiency is a measure used to describe the effectiveness of information transfer between nodes within a network. It is a valuable tool for characterizing the overall organization and function of brain networks based on random walks. Two types of efficiencies are commonly computed: global efficiency and local efficiency.

Global efficiency is a measure of the network's overall ability to transfer information between any pair of nodes (Latora and Marchiori 2001). To calculate global efficiency, we the MFPT between all pairs of nodes in the network. MFPT is the average number of steps a random walker takes to reach a target node from a starting node for the first time (Hughes 1995)r. For a network with N nodes, the MFPT is calculated using the transition probabilities between nodes, which are dependent on the connection strengths and the differences in node activities at each time step (equations (1)-(4)). Once the MFPT matrix is computed, the inverse of the MFPT between each pair of nodes is taken (excluding the diagonal elements). The global efficiency is then calculated as the average of these inverse MFPT values, normalized by the total number of possible node pairs $\left(N(N-1)\right)$. Higher global efficiency values indicate better overall integration of the network, reflecting a more efficient information transfer between nodes.

Local efficiency, on the other hand, is a measure of the network's fault tolerance or resilience to the removal of a node. It represents the efficiency of the information transfer between the neighbors of a given node when that node is removed from the network. To compute local efficiency, first, we identify the neighbors of each node (i.e., the nodes directly connected to it). Then, extract the subgraph MFPT matrix of these neighbors, and calculate the inverse of the MFPT between each pair of neighbors. The local efficiency of the node is the average of these inverse MFPT values, normalized by the total number of possible neighbor pairs. The average of local efficiencies across all nodes in the network is often reported as an overall measure of segregation in the network (Latora and Marchiori 2001).

Results

A large number of random walkers (10^4) were randomly placed on each of the 491 correlation-based functional connectivity matrices and allowed to move for $T = 1000$. At each time step, the walkers moved randomly between directly connected nodes, with the probability depending on the number of walkers at each node and the strength and sign of the connections (see equations (1)-(4)). We recorded the number of walkers in each node (i.e., $A(i,t)$) and the number of walkers that transited through each connection at each time step. This allowed us to compute the Walkers' connectivity matrix(W), where each connection represents the total number of walkers that transited through that connection during the entire simulation. Note that (W) is a non-symmetric matrix. For comparison, we also ran a simulation with a classical

random walk where the transition probability only depended on the absolute value of the connections: $P_{ij}(t) = |C_{ij}| / \sum_{j=1}^{N} |C_{ij}|$.

Figure 1 shows the correlation-based functional connectivity matrix for one subject (Figure 1A), and the corresponding walkers' activity on each node ($A(i,t)$) in the network when using the absolute value of the connections (Figure 1B), and for the signed case (Figure 1C). We can see from the figure that for the signed case, the activities in the nodes exhibit more variability than for the 'Abs' case. This suggests that considering signed connections may provide a more nuanced understanding of the network dynamics.

Figure 2 displays the walkers' connectivity matrix W, averaged across subjects for both the 'abs' case (Figure 2A) and the signed case (Figure 2B). We also plotted histograms of the connections in W for the 'Abs' (Figure 2C) and signed cases (Figure 2D). In the 'Abs' case, we observed 11,523 connections with fewer than 1,000 walkers, more than the 10,972 connections in the signed network. For highly transited connections, the 'Abs' case had only four connections with over 3,000 walkers and none with more than 5,000 walkers. In contrast, the signed case featured 270 connections with over 3,000 walkers and eight connections with more than 5,000 walkers. The signed case revealed a greater number of highly transited connections and demonstrated the presence of highly transited connections between homologous regions in the left and right hemispheres. Specifically, the eight highly transited connections, in descending order, were: 1) 'Calcarine L' to 'Calcarine R', 2) 'Calcarine R' to 'Calcarine L', 3) 'Cerebellum 8 L' to 'Cerebellum 7b L', 4) 'Cerebellum 7b L' to 'Cerebellum 8 L', 5) 'Cuneus R' to 'Cuneus L', 6) 'Cuneus L' to 'Cuneus R', 7) 'Temporal Sup R' to 'Temporal Sup L', and 8) 'Temporal Sup L' to 'Temporal Sup R'. Here, 'L' denotes the left brain hemisphere, and 'R' indicates the right

Figure 3 shows the total number of walkers that transited each brain area, averaged across all subjects. In the 'Abs' case (Figure 3A), the most transited brain areas were 'Temp Inf L', 'Lingual R', and 'Temporal pole Mid L'. Interestingly, for the signed network (Figure 3B), the most transited area was also 'Temp Inf L', followed by 'Temporal pole Mid L'. 'Lingual L', which ranked as the second most transited area in the 'Abs' network, dropped to the 17th position in the signed case. This result highlights the differences in the most transited brain areas between the 'Abs' and signed cases, demonstrating the impact of considering both positive and negative connections on the analysis.

Figure 4 compares the global efficiency (Figure 4A), local efficiency (Figure 4B), and MFPT (Figure 4C) averaged across subjects between the 'Abs' and signed cases. Figure 4C demonstrates that taking the absolute value of the connections leads to an underestimation of the MFPT. As we calculated the efficiencies using MFPT, this resulted in an overestimation of their values. An interesting question in the signed case concerns the impact of the number of walkers in the negative connections on the calculated topological measures. Figures 4D, 4E, and 4F plot the three topological measures against the fraction of walkers that transited negative connections compared to positive connections (Neg/Pos fraction). We found significant correlations between global efficiency ($r = 0.59,\ p = 10^{-47}$), local efficiency ($r = 0.86, p = 10^{-142}$), and MFPT ($r = 0.85\ , p = 10^{-136}$) with the Neg/Pos fraction.

Insert Figure 1 around here

Insert Figure 2 around here

Insert Figure 3 around here

Insert Figure 4 around here

Discussion

In this study, we introduced an adaptive random walk approach for analyzing correlation-based brain networks, taking into account both positive and negative connections. The proposed method captures a broader range of network interactions and dynamics, revealing patterns that might be missed when employing traditional methods. Our results indicate that the classical random walk approach, which relies on the absolute value of connections, overestimates network integration and segregation while underestimating the mean first passage time (MFPT) compared to the proposed adaptive random walk model. This has important implications for understanding the interregional coordination underlying various cognitive processes and behaviors (Bassett and Sporns 2017).

Despite the advantages of the adaptive random walk model, there are some limitations that should be addressed in future research. One limitation is the reliance on static functional connectivity matrices, which may not fully capture the dynamic nature of brain activity. Future studies could extend the model to account for dynamic functional connectivity, allowing for the investigation of time-varying network organization (Preti, Bolton, and Van De Ville 2017). Another limitation is the potential sensitivity of the model to the choice of parameters, such as the initial number of walkers and the number of time steps. A systematic exploration of these parameters should be performed to determine their impact on the results and to identify optimal settings for different applications.

An additional aspect to consider in our study is the use of GSR in preprocessing the neuroimaging data. GSR is a common preprocessing step that aims to remove global confounds, such as physiological noise, from the data (Murphy and Fox 2017). However, it has been shown that GSR can introduce more negative correlations into the functional connectivity matrices (Murphy et al. 2009). This has led to some debate regarding the validity of negative correlations as they may, at least partially, be an artifact of the preprocessing technique (Saad et al. 2012). The potential impact of GSR on our adaptive random walk model is an important consideration, as it could affect the observed transition probabilities and the subsequent network measures. In our analysis, we treated both positive and negative correlations as meaningful connections, reflecting the underlying physiological mechanisms. However, if GSR artificially inflates the number of negative correlations, it could bias our results, potentially leading to an overestimation

of the impact of negative connections on the network organization. To address this issue, future research could explore alternative preprocessing techniques that do not introduce additional negative correlations or investigate the sensitivity of the adaptive random walk model to the presence of artificially induced negative correlations. Comparing the results obtained using different preprocessing methods or incorporating additional steps to correct for the possible effects of GSR could help to disentangle the true physiological significance of the negative correlations from the potential artifacts introduced by GSR. This would contribute to a more robust understanding of the brain network organization and its underlying functional interactions.

Finally, future research could also further refine the adaptive random walk model by incorporating additional factors that may influence the transition probabilities, such as the spatial distance between brain regions or the directionality of connections.

Conclusions

In conclusion, the adaptive random walk model presented in this study offers a promising approach for the analysis of correlation-based brain networks, accounting for both positive and negative connections. While there are limitations to the current model, addressing these in future research will help to further enhance its applicability and utility. This method provides a more comprehensive understanding of brain network organization and has the potential to advance our knowledge of the complex interplay between brain regions in various cognitive processes and behaviors.

References

Avants, Brian B., Nicholas J. Tustison, Gang Song, Philip A. Cook, Arno Klein, and James C. Gee. 2011. "A Reproducible Evaluation of ANTs Similarity Metric Performance in Brain Image Registration." *NeuroImage* 54 (3): 2033–44. https://doi.org/10.1016/j.neuroimage.2010.09.025.

Bassett, Danielle S., and Olaf Sporns. 2017. "Network Neuroscience." *Nature Neuroscience* 20 (3): 353–64. https://doi.org/10.1038/nn.4502.

Behzadi, Yashar, Khaled Restom, Joy Liau, and Thomas T. Liu. 2007. "A Component Based Noise Correction Method (CompCor) for BOLD and Perfusion Based FMRI." *NeuroImage* 37 (1): 90–101. https://doi.org/10.1016/j.neuroimage.2007.04.042.

Bressler, Steven L., and Vinod Menon. 2010. "Large-Scale Brain Networks in Cognition: Emerging Methods and Principles." *Trends in Cognitive Sciences* 14 (6): 277–90. https://doi.org/10.1016/j.tics.2010.04.004.

Bullmore, Ed, and Olaf Sporns. 2009. "Complex Brain Networks: Graph Theoretical Analysis of Structural and Functional Systems." *Nature Reviews Neuroscience* 10 (3): 186–98. https://doi.org/10.1038/nrn2575.

Cameron, Craddock, Sikka Sharad, Cheung Brian, Khanuja Ranjeet, Ghosh Satrajit, Yan Chaogan, Li Qingyang, et al. 2013. "Towards Automated Analysis of Connectomes: The

Configurable Pipeline for the Analysis of Connectomes (C-PAC).” *Frontiers in Neuroinformatics* 7. https://doi.org/10.3389/conf.fninf.2013.09.00042.

Cameron, Craddock, Benhajali Yassine, Chu Carlton, Chouinard Francois, Evans Alan, Jakab András, Khundrakpam Budhachandra, et al. 2013. “The Neuro Bureau Preprocessing Initiative: Open Sharing of Preprocessed Neuroimaging Data and Derivatives.” *Frontiers in Neuroinformatics* 7. https://doi.org/10.3389/conf.fninf.2013.09.00041.

Cox, Robert W. 1996. “AFNI: Software for Analysis and Visualization of Functional Magnetic Resonance Neuroimages.” *Computers and Biomedical Research* 29 (3): 162–73. https://doi.org/10.1006/cbmr.1996.0014.

Friston, Karl J. 1994. “Functional and Effective Connectivity in Neuroimaging: A Synthesis.” *Human Brain Mapping* 2 (1–2): 56–78. https://doi.org/10.1002/hbm.460020107.

Grabner, Günther, Andrew L. Janke, Marc M. Budge, David Smith, Jens Pruessner, and D. Louis Collins. 2006. “Symmetric Atlasing and Model Based Segmentation: An Application to the Hippocampus in Older Adults.” *Medical Image Computing and Computer-Assisted Intervention: MICCAI ... International Conference on Medical Image Computing and Computer-Assisted Intervention* 9 (Pt 2): 58–66. https://doi.org/10.1007/11866763_8.

Heuvel, Martijn P. van den, and Hilleke E. Hulshoff Pol. 2010. “Exploring the Brain Network: A Review on Resting-State FMRI Functional Connectivity.” *European Neuropsychopharmacology* 20 (8): 519–34. https://doi.org/10.1016/j.euroneuro.2010.03.008.

Hughes, Barry D. 1995. *Random Walks and Random Environments*. Oxford, New York: Oxford University Press.

Kazeminejad, Amirali, and Roberto C. Sotero. 2019. “Topological Properties of Resting-State FMRI Functional Networks Improve Machine Learning-Based Autism Classification.” *Frontiers in Neuroscience* 12. https://www.frontiersin.org/articles/10.3389/fnins.2018.01018.

Latora, Vito, and Massimo Marchiori. 2001. “Efficient Behavior of Small-World Networks.” *Physical Review Letters* 87 (19): 198701. https://doi.org/10.1103/PhysRevLett.87.198701.

Mahadevan, Arun S., Ursula A. Tooley, Maxwell A. Bertolero, Allyson P. Mackey, and Danielle S. Bassett. 2021. “Evaluating the Sensitivity of Functional Connectivity Measures to Motion Artifact in Resting-State FMRI Data.” *NeuroImage* 241 (November): 118408. https://doi.org/10.1016/j.neuroimage.2021.118408.

Mazziotta, John, Arthur Toga, Alan Evans, Peter Fox, Jack Lancaster, Karl Zilles, Roger Woods, et al. 2001. “A Four-Dimensional Probabilistic Atlas of the Human Brain.” *Journal of the American Medical Informatics Association* 8 (5): 401–30. https://doi.org/10.1136/jamia.2001.0080401.

Meszlényi, Regina J., Petra Hermann, Krisztian Buza, Viktor Gál, and Zoltán Vidnyánszky. 2017. “Resting State FMRI Functional Connectivity Analysis Using Dynamic Time Warping.” *Frontiers in Neuroscience* 11. https://www.frontiersin.org/articles/10.3389/fnins.2017.00075.

Murphy, Kevin, Rasmus M. Birn, Daniel A. Handwerker, Tyler B. Jones, and Peter A. Bandettini. 2009. “The Impact of Global Signal Regression on Resting State Correlations: Are Anti-Correlated Networks Introduced?” *NeuroImage* 44 (3): 893–905. https://doi.org/10.1016/j.neuroimage.2008.09.036.

Murphy, Kevin, and Michael D. Fox. 2017. "Towards a Consensus Regarding Global Signal Regression for Resting State Functional Connectivity MRI." *NeuroImage* 154 (July): 169–73. https://doi.org/10.1016/j.neuroimage.2016.11.052.

Noh, Jae Dong, and Heiko Rieger. 2004. "Random Walks on Complex Networks." *Physical Review Letters* 92 (11): 118701. https://doi.org/10.1103/PhysRevLett.92.118701.

Pearson, Karl. 1905. "The Problem of the Random Walk." *Nature* 72 (1867): 342–342. https://doi.org/10.1038/072342a0.

Preti, Maria Giulia, Thomas AW Bolton, and Dimitri Van De Ville. 2017. "The Dynamic Functional Connectome: State-of-the-Art and Perspectives." *NeuroImage*, Functional Architecture of the Brain, 160 (October): 41–54. https://doi.org/10.1016/j.neuroimage.2016.12.061.

Riascos, A P, and José L Mateos. 2021. "Random Walks on Weighted Networks: A Survey of Local and Non-Local Dynamics." *Journal of Complex Networks* 9 (5): cnab032. https://doi.org/10.1093/comnet/cnab032.

Rubinov, Mikail, and Olaf Sporns. 2011. "Weight-Conserving Characterization of Complex Functional Brain Networks." *NeuroImage* 56 (4): 2068–79. https://doi.org/10.1016/j.neuroimage.2011.03.069.

Saad, Ziad S., Stephen J. Gotts, Kevin Murphy, Gang Chen, Hang Joon Jo, Alex Martin, and Robert W. Cox. 2012. "Trouble at Rest: How Correlation Patterns and Group Differences Become Distorted After Global Signal Regression." *Brain Connectivity* 2 (1): 25–32. https://doi.org/10.1089/brain.2012.0080.

Smith, Stephen M., Mark Jenkinson, Mark W. Woolrich, Christian F. Beckmann, Timothy E. J. Behrens, Heidi Johansen-Berg, Peter R. Bannister, et al. 2004. "Advances in Functional and Structural MR Image Analysis and Implementation as FSL." *NeuroImage* 23 Suppl 1: S208-219. https://doi.org/10.1016/j.neuroimage.2004.07.051.

Sotero, Roberto C., Lazaro M. Sanchez-Rodriguez, Narges Moradi, and Mehdy Dousty. 2020. "Estimation of Global and Local Complexities of Brain Networks: A Random Walks Approach." *Network Neuroscience* 4 (3): 575–94. https://doi.org/10.1162/netn_a_00138.

Tzourio-Mazoyer, N., B. Landeau, D. Papathanassiou, F. Crivello, O. Etard, N. Delcroix, B. Mazoyer, and M. Joliot. 2002. "Automated Anatomical Labeling of Activations in SPM Using a Macroscopic Anatomical Parcellation of the MNI MRI Single-Subject Brain." *NeuroImage* 15 (1): 273–89. https://doi.org/10.1006/nimg.2001.0978.

Wan, Cong, Yanhui Fang, Cong Wang, Yanxia Lv, Zejie Tian, and Yun Wang. 2019. "SignRank: A Novel Random Walking Based Ranking Algorithm in Signed Networks." *Wireless Communications and Mobile Computing* 2019 (April): e4813717. https://doi.org/10.1155/2019/4813717.

Yang, Bo, William Cheung, and Jiming Liu. 2007. "Community Mining from Signed Social Networks." *IEEE Transactions on Knowledge and Data Engineering* 19 (10): 1333–48. https://doi.org/10.1109/TKDE.2007.1061.

Zhou, Jianlin, Lingbo Li, An Zeng, Ying Fan, and Zengru Di. 2018. "Random Walk on Signed Networks." *Physica A: Statistical Mechanics and Its Applications* 508 (October): 558–66. https://doi.org/10.1016/j.physa.2018.05.139.

Figures

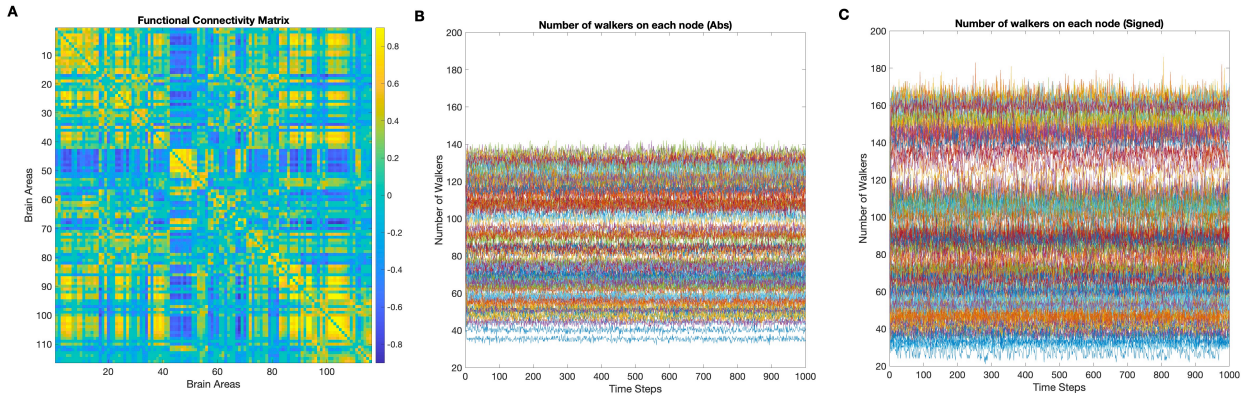

Figure 1. Correlation-based functional connectivity matrix and walkers' activity on each node in the network for one subject. (A) Functional connectivity matrix illustrating the strength of correlations between different brain regions for a single subject. (B) Walker activity (A(i,t)) on each node in the network when using the absolute value of the connections, demonstrating relatively uniform activity across nodes. (C) Walker activity (A(i,t)) on each node in the network for the signed case, displaying increased variability in node activity compared to the absolute case.

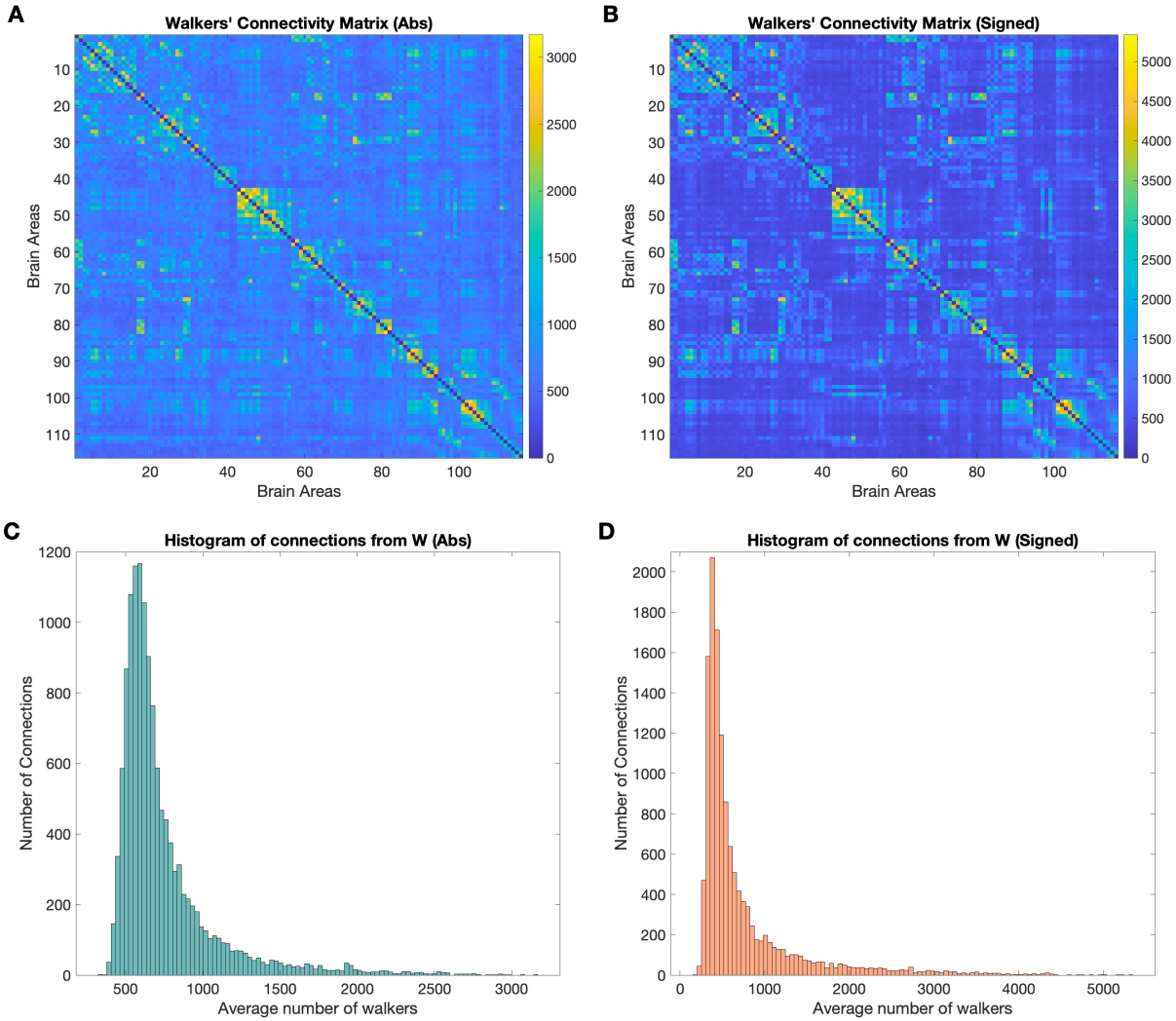

Figure 2: Comparison of walkers' connectivity matrices and connection histograms for the 'Abs' and signed cases. (A) Walkers' connectivity matrix W, averaged across subjects for the 'Abs' case, illustrating the number of walkers transiting between different brain regions using the absolute value of the connections. (B) Walkers' connectivity matrix W, averaged across subjects for the signed case. (C) Histogram of connections in W for the 'Abs' case, showing the distribution of connections with different numbers of walkers. (D) Histogram of connections in W for the signed case, with a greater number of highly transited connections than the 'Abs' case.

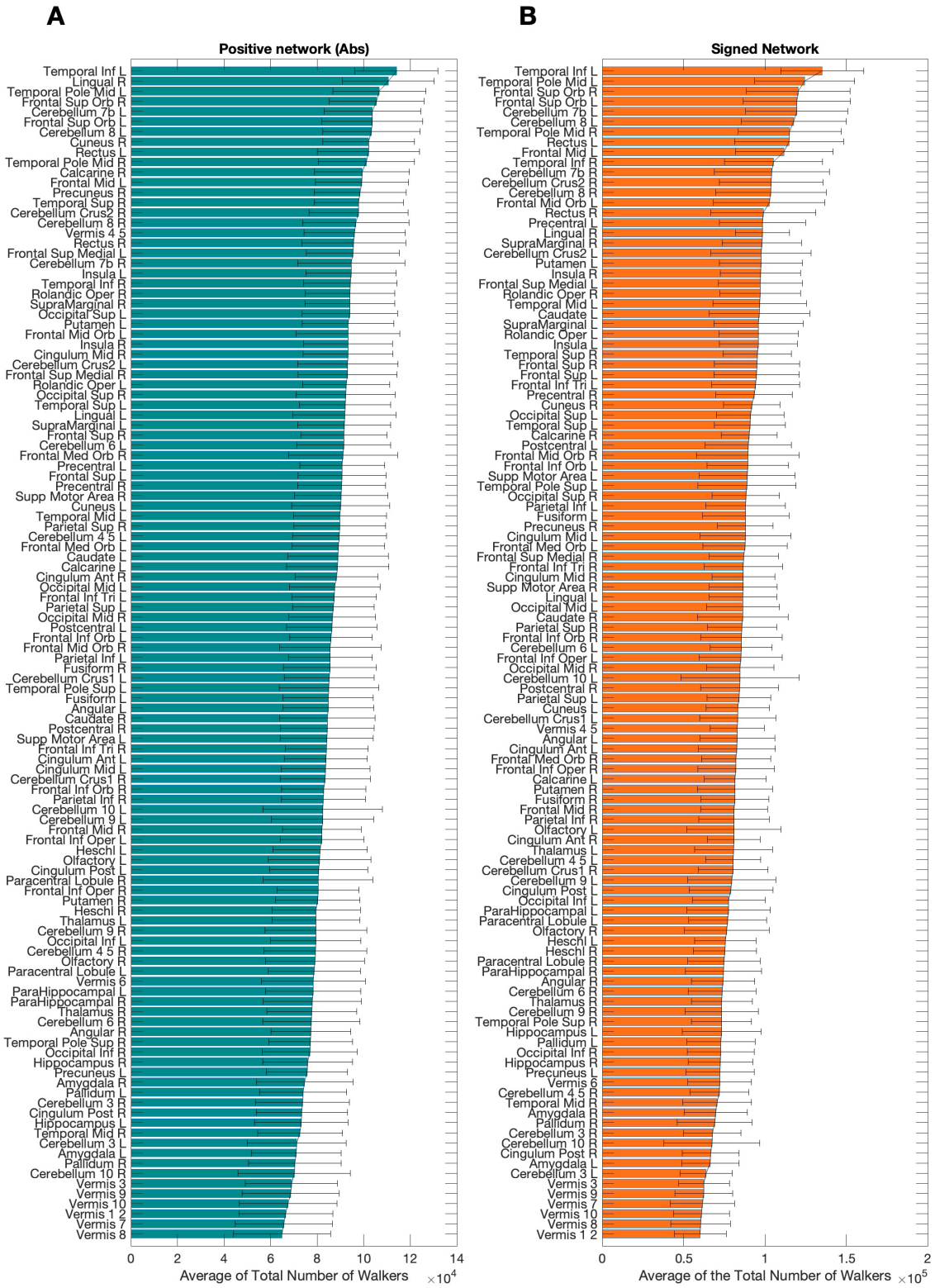

Figure 3: Total number of walkers transiting each brain area, averaged across all subjects for the 'Abs' and signed cases. (A) Bar plot showing the mean and standard deviation of walkers transiting each brain area

in the 'Abs' case. (B) Bar plot illustrating the mean and standard deviation of walkers transiting each brain area in the signed case.

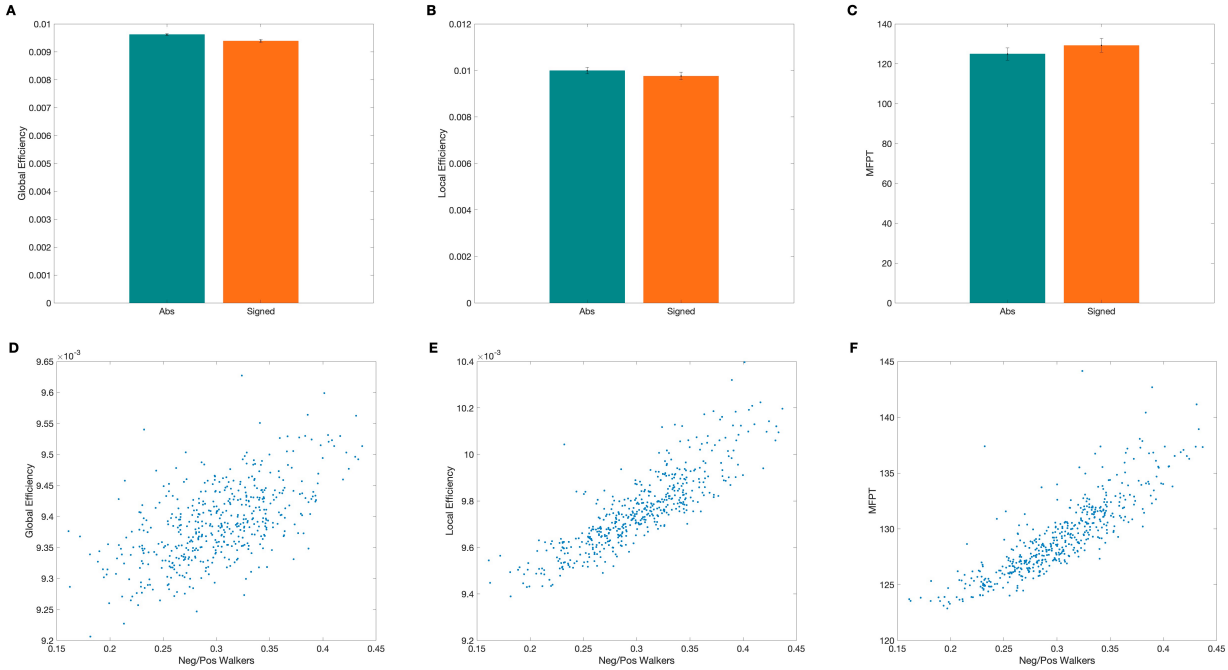

Figure 4: Computing topological measures with random walks. Comparison of global efficiency, local efficiency, and MFPT between the 'Abs' and signed cases, and their correlation with the fraction of walkers transiting negative connections vs positive connections (Neg/Pos fraction). (A) Global efficiency comparison, (B) local efficiency comparison, and (C) MFPT comparison between, (D) Scatter plot of the relationship between global efficiency and Neg/Pos fraction, with a significant correlation ($r = 0.59,\ p = 10^{-47}$),. (E) Scatter plot illustrating the correlation between local efficiency and the Neg/Pos fraction ($r = 0.86, p = 10^{-142}$). (F) Scatter plot depicting the correlation between MFPT and the Neg/Pos fraction ($r = 0.85\ , p = 10^{-136}$).